ACS Macro Letters

Letter

pubs.acs.org/macroletters

Iron Oxide Nanoparticles Grafted with Sulfonated and Zwitterionic Polymers: High Stability and Low Adsorption in Extreme Aqueous Environments

Edward L. Foster,[†,‡] Zheng Xue,[‡,§] Clarissa M. Roach,[†] Eric S. Larsen,[†] Christopher W. Bielawski,[†] and Keith P. Johnston*[,§]

[†]Department of Chemistry and [§]Department of Chemical Engineering, University of Texas at Austin, Austin, Texas 78712, United States

Supporting Information

ABSTRACT: A facile "grafting through" approach was developed to tether tunable quantities of poly(2-acrylamido-2-methylpropanesulfonic acid) (PAMPS) as well as zwitterionic poly([3-(methacryloylamino)propyl]dimethyl(3-sulfopropyl)ammonium hydroxide) (PMPDSA) homopolymer onto iron oxide (IO) nanoparticles (NPs). In this case, homopolymers may be grafted, unlike "grafting to" approaches that often require copolymers containing anchor groups. The polymer coating provided steric stabilization of the NP dispersions at high salinities and elevated temperature (90 °C) and almost completely prevented adsorption of the NPs on silica microparticles and crushed Berea sandstone. The adsorption of PAMPS IO NPs decreased with the polymer loading, whereby the magnitude of the particle-surface electrosteric repulsion increased. The zwitterionic PMPDSA IO NPs displayed 1 order of magnitude less adsorption onto crushed Berea sandstone relative to the anionic PAMPS IO NPs. The ability to design homopolymer coatings on nanoparticle surfaces by the "grafting through" technique is of broad interest for designing stable dispersions and modulating the interactions between nanoparticles and solid surfaces.

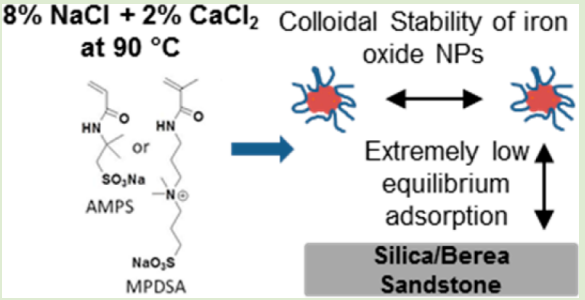

Recent efforts have been directed toward the development of superparamagnetic iron oxide (IO) nanoparticles (NPs) that are stable in American Petroleum Institute (API) brine (8 wt %/wt NaCl + 2 wt %/wt $CaCl_2$, anhydrous basis) for subsurface oil field applications.[1−4] Building on the established utility of superparamagnetic IO NPs as contrast agents in biomedical MRI imaging,[5,6] similar materials may find uses in subsurface applications including electromagnetic hydraulic fracture diagnostics, well logging, and cross-well electromagnetic tomography.[7−9] For various imaging applications, the NPs must remain stable against aggregation and transport through the reservoir rock without significant retention. Although a large number of NPs stabilizers have been developed for such purposes, the extreme environments found in oil reservoirs, including high salinities (>1 M), the presence of divalent salts (Ca^{2+} and Mg^{2+}), and high temperature (90−150 °C), often lead to NP aggregation and adsorption on mineral surfaces, and ultimately hinders transport.[10]

To date, our research efforts have focused on stabilizing IO NPs by grafting or adsorbing statistical copolymers of 2-acrylamido-2-methylpropanesulfonic acid (AMPS) and acrylic acid (AA), which serve as stabilizer and anchoring groups, respectively. In the AMPS-based stabilizers, the highly acidic sulfonate groups exhibit low Ca^{2+} binding affinities while the hydrophilic amide groups facilitate hydration; thus, the corresponding homopolymer (i.e., PAMPS) remains soluble even at high salinities and temperatures.[1,11,12] The addition of AA to the aforementioned homopolymer allows for covalent grating of the polymer to IO functionalized with surface amine groups. The amine groups were formed with aminopropyltriethoxysilane (APTES) and the formation of amide bonds between amines and AA groups was catalyzed with 1-ethyl-3-(3-(dimethylamino)propyl) carbodiimide (EDC) hydrochloride. Using this method, the amine-coated IO NPs were permanently linked to AA groups on the copolymer. A rapid batch technique developed recently[1] was used to determine the equilibrium adsorption of the aforementioned NPs on silica microspheres, as well as crushed Berea sandstone microparticles.[2,3]

In parallel, we and others have been exploring the utility of another class of polymers stable to high salinities and elevated temperatures in oil field applications: the zwitterionic sulfobetaine polymers ([3-(methacryloylamino)propyl]-dimethyl(3-sulfopropyl)ammonium hydroxide (MPDSA)). To date, several types of zwitterionic polymers, such as phosphobetaine,[13] sulfobetaine,[14,15] and carboxybetaine,[16,17]

Received: July 11, 2014
Accepted: August 14, 2014
Published: August 18, 2014

   dx.doi.org/10.1021/mz5004213 | ACS Macro Lett. 2014, 3, 867−871

Scheme 1. Synthesis of Either PAMPS or PMPDSA via the "Grafting through" Technique

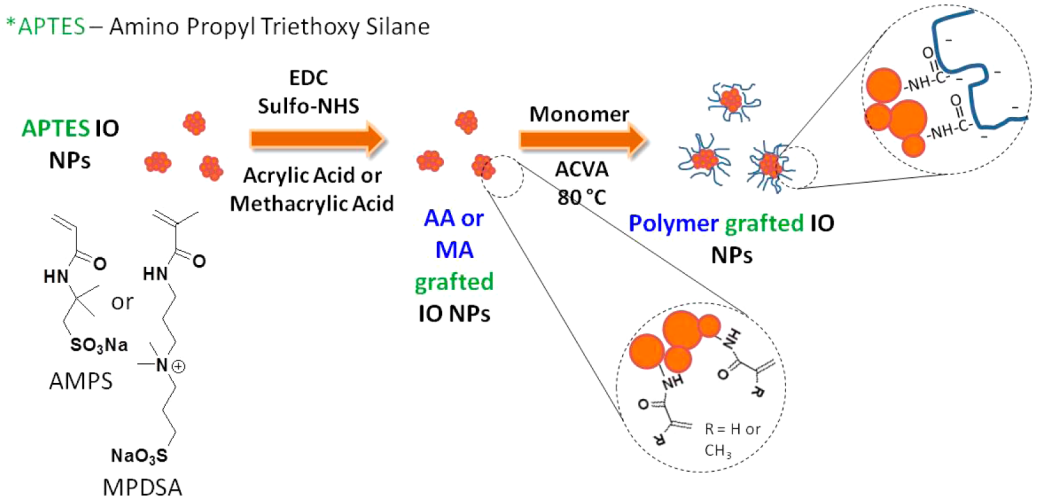

have been investigated for applications as biosensors,[18−20] enzyme immobilization,[21] soft contact lenses,[22,23] drug release,[24,25] and nonfouling materials.[26−28] When grafted onto NPs, it is expected that the stable and extended zwitterionic polymer will provide robust colloidal stability of the corresponding NPs. However, despite this potential, studies that evaluate their ability to stabilize IO NPs have yet to be performed.

Typically polymer-functionalized NPs are prepared using a "grafting from" method, where initiators are tethered to the surface of the NPs, and catalysts are used to grow polymer. Unfortunately, because numerous steps and expensive reagents are often required, the approach is not commonly used in industrial-scale processes.[29] To overcome these challenges, we developed a facile "grafting through" technique to graft PAMPS or PMPDSA to IO NPs. The "grafting through" technique works by first functionalizing the surface of the NP with polymerizable moieties , that is, vinyl groups (Scheme 1), followed by aqueous free radical polymerization of monomers in the presence of the vinyl coated NP. During this process, the propagating polymer grafts through the vinyl groups tethered to the NP.[30−32] Moreover, the approach allows the amount of polymer grafted to the IO NPs to be effectively tuned via controlling the concentration of feed monomers, that is, 0.48, 0.97, 1.5, and 1.9 M ($PAMPS_1$, $PAMPS_2$, $PAMPS_3$, $PAMPS_4$ IO NPs, respectively) while maintaining the IO NPs and initiator concentrations. Finally, these polymer-grafted IO NPs were found to display robust colloidal stabilities in API brine at 90 °C for over 1 week and low adsorption on silica and crushed Berea sandstone.

Grafting of acrylic acid to amine-functionalized IO NP (APTES IO NP) and "grafting through" of AMPS monomer: Silane coupling agent APTES was used to introduce amine groups to bare iron oxide NPs (Figure S1). The synthesis of the amine-functionalized IO NPs (APTES IO NPs) was prepared according to previous reports and characterized using ATR-IR spectroscopy, thermogravimetric analysis (TGA; Figure 1b), and dynamic light scattering (DLS; see Figure 1 and the Supporting Information). After synthesis of the APTES IO NPs, acrylic acid (AA) was grafted to the amines via an EDC/Sulfo-NHS facilitated amidation reaction, as summarized in Scheme 1. From the ATR-IR data, it was evident when comparing the APTES IO NPs to the AA IO NPs, a new signal at 1714 cm^{-1} was observed. This peak suggested that a grafted amide bond was successfully formed. In addition, the hydrodynamic diameter (D_H; pH 5 in deionized (DI) water) of APTES IO NP increased from ∼85 ± 8 to ∼140 ± 17 nm for AA IO NPs under otherwise identical conditions.

The AMPS monomer at various concentrations was then grafted to the IO NPs via aqueous free radical polymerization to prepare the PAMP IO NPs. As shown in Figure 1a, the signals at 1656 and 1560 cm^{-1}, which were attributed to the −C═O and −N−H groups of the PAMPS IO NPs, increased in intensity when compared to AA IO NPs, indicating successful preparation of PAMPS grafted nanoparticles ($PAMPS_{1-4}$ IO NPs).[33,34]

In parallel, the PAMPS content of the PAMPS IO NPs was investigated by TGA. As shown in Figure 1b, the respective PAMPS weight fractions for the PAMPS IO NPs prepared at various concentrations were measured to be 17, 29, 35, and 40% at 600 °C for the $PAMPS_1$, $PAMPS_2$, $PAMPS_3$, and $PAMPS_4$ ($PAMPS_{1-4}$) IO NPs, respectively, and the magnitude of the ζ potentials increased monotonically: −35 ± 3, −45 ± 4, −60 ± 2, and −67 ± 3 mV (at pH 8). Thus, the "grafting through" technique provided excellent control of the grafting amount and surface charge.

In addition, D_H shows that despite the monomer feed ratios, the $PAMPS_{1-3}$ IO NPs of similar sizes are obtained. It should be noted, however, that D_H increased from ∼140 ± 17 nm for the AA IO NPs to ∼200 nm for $PAMPS_{1-3}$ IO NPs and ∼243 ± 19 nm in the case of $PAMPS_4$ IO NPs. Presumably, the grafting process led to aggregation of clusters since multiple vinyl functionalized NPs (AA IOs or MA IOs) may be bridged by growing polymer chains during polymerization. Regardless of the increase in D_H, the $PAMPS_{1-4}$ IO NPs formed stable colloidal dispersions in API brine at room temperature as well as 90 °C. The stability was studied by measuring the D_H in API brine at 90 °C for 1 week, which remained at a constant size for the entire series studied (see Figure S2). Solid precipitate was not observed. Collectively, these data demonstrate that the $PAMPS_{1-4}$ IO NPs remain electrosterically stabilized under extreme salinities and temperatures.

Static batch adsorption of $PAMPS_{1-4}$ IO NPs: A series of equilibrium batch adsorption tests of the IO NPs was performed on silica microspheres as well as crushed Berea sandstone at various feed IO concentrations. The results were

dx.doi.org/10.1021/mz5004213 | ACS Macro Lett. 2014, 3, 867−871

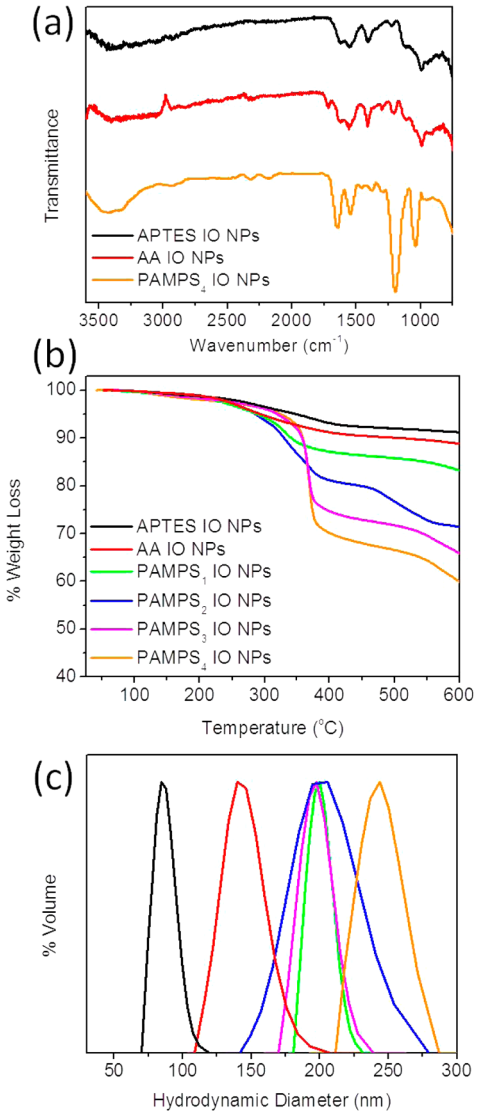

Figure 1. (a) ATR-IR spectra of APTES IO NPs, AA IO NPs, and the $PAMPS_4$ IO NPs. (b) TGA spectra of various stages of IO NP functionalization. (c) Volume-weighted D_H distribution of APTES IO NPs in DI water, and PAMPS grafted IO NPs in API brine at pH 8. (Note: the legend shown in (b) corresponds to the same materials described in (c).)

observed visually (Figure 2a–d) and quantified via material balance (Tables 1 and 2). It is clearly seen based on the color of the supernatant that fewer IO NPs were adsorbed to the silica microspheres and crushed Berea sandstone in the case of the $PAMPS_4$ IO NPs when compared to the $PAMPS_1$ IO NPs at all three initial concentrations. Despite the high ionic strength and potential for Ca^{2+} bridging of the anionic carboxylate/sulfonate groups to the anionic silica sites, the adsorption levels were remarkably low.

As the PAMPS loading on the IO NPs increased (from $PAMPS_{1-3}$ IO NPs), the specific adsorption decreased by 1 order of magnitude (Table 1). However, a further increase in loading ($PAMPS_{3-4}$ IO NPs) did not decrease the specific adsorption. The specific adsorption in API brine of the $PAMPS_4$ IO NPs (initial concentration of 0.1% w/v) was 0.02 ± 0.02 mg/m^2, which corresponds to low monolayer coverage of 0.004%. The low adsorption for $PAMPS_{3-4}$ IO NPs suggested to us that the polymer remains solvated so that

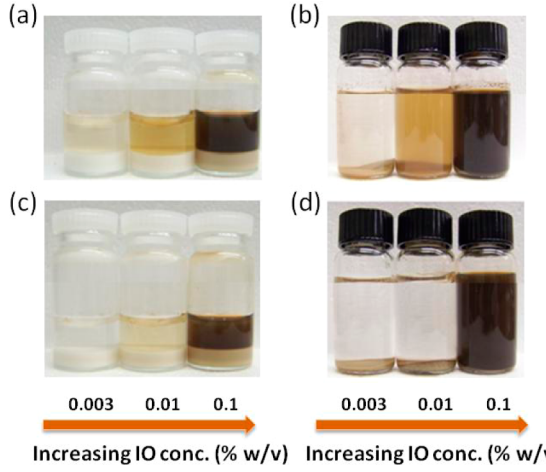

Figure 2. Photographs of (a) $PAMPS_4$ IO NPs on silica microsphere and (b) crushed Berea sandstone. (c) $PAMPS_1$ IO NPs on silica microsphere and (d) crushed Berea sandstone in API brine at IO concentrations from 0.003 to 0.1% w/v. Each vial contains 10 mL of IO dispersion at pH 8 and 1 g silica microspheres or 200 mg crushed Berea sandstone and was equilibrated for 16–20 h.

extended chains on the surface provide sufficient steric repulsion with the anionic silica.[35]

To provide a more severe test of nanoparticle interactions with solid surfaces, we studied NP adsorption on crushed Berea sandstone with (~7% by weight) clay minerals that undergo cation exchange. Unlike silica microspheres with relatively uniform negatively charged surfaces, Berea sandstone contains positively charged sites on the edges of the clay. As summarized in Table 2, PAMPS on the NP surface provided sufficient electrosteric repulsion to result in adsorption less than 1% of monolayer coverage in each case. In most cases, a decrease in adsorption with PAMPS loading was observed from $PAMPS_1$ to $PAMPS_{2-3}$ IO NPs. At all concentrations for the PAMPS series, the specific adsorption values were higher for crushed Berea sandstone relative to the silica microspheres, consistent with the positive sites that attract the anionic nanoparticles.

Zwitterionic coated (MPDSA) IO NPs, characterization, and batch testing: To further attempt to achieve low adsorption on crushed Berea sandstone, we decided to investigate zwitterionic polymers. Efforts were directed toward polymeric forms of ([3-(methacryloylamino)propyl]dimethyl(3-sulfopropyl)-ammonium hydroxide (MPDSA) as such zwitterionic species are currently being used in oil field applications, including enhanced oil recovery and drilling fluids.[36–38] In addition, the negative sulfonate and the inner tertiary ammonium groups were expected to provide charge balance for the positively charged edges of clays in crushed Berea sandstone while resisting undesired cation exchange.

Grafting of methacrylic acid (MA) to APTES IO NP and "grafting through" of MPDSA: For the "grafting through" using the MPDSA monomer, the first step involved grafting methacrylic acid (MA) to the surface of the APTES IO NPs via a EDC/Sulfo-NHS mediation amidation (Scheme 1). The MA grafted IO NPS (MA IO NPs) were then characterized using ATR-IR spectroscopy and DLS (Figures S2 and S3, respectively). Upon the successful synthesis and characterization of the MA IO NPs, the MPDSA monomer (1.4 M) was then polymerized in the presence of the MA IO NPs to graft the polymer to the IO NPs. In parallel, the PMPDSA content of the PMPDSA IO NPs was evaluated by TGA and measured

dx.doi.org/10.1021/mz5004213 | ACS Macro Lett. 2014, 3, 867–871

Table 1. Adsorption of $PAMPS_{1-4}$ IO NPs on 8 μm Silica Microspheres in API Brine at pH 8 at Different IO Concentrations[a]

polymer coating	initial IO concn (% w/v)	% IO adsorbed	final eq IO concn (% w/v)	specific adsorption[b] (mg IO/m^2)	% monolayer
$PAMPS_1$ IO NPs	0.003	95.3	0.0001	0.10 ± 0.02	0.019
	0.01	67.4	0.0032	0.23 ± 0.02	0.045
	0.1	24.5	0.0754	0.84 ± 0.06	0.16
$PAMPS_2$ IO NPs	0.003	27.4	0.0021	0.030 ± 0.002	0.006
	0.01	10.6	0.0044	0.040 ± 0.003	0.007
	0.1	2.8	0.0479	0.140 ± 0.02	0.027
$PAMPS_3$ IO NPs	0.003	9.3	0.0027	0.010 ± 0.01	0.002
	0.01	1.8	0.0098	0.030 ± 0.01	0.006
	0.1	0.9	0.0991	0.040 ± 0.04	0.008
$PAMPS_4$ IO NPs	0.003	8.1	0.0027	0.010 ± 0.01	0.001
	0.01	5.8	0.0094	0.020 ± 0.01	0.003
	0.1	0.7	0.0993	0.020 ± 0.02	0.004

[a]The specific surface area of colloidal silica was measured to be ~0.5825 m^2/g via BET methods. [b]Average of four independent experiments; uncertainty in specific adsorption based on error propagation analysis.

Table 2. Adsorption of $PAMPS_{1-4}$ IO NPs on Crushed Berea Sandstone in API Brine at pH 8 at Different IO Concentrations[a]

polymer coating	initial IO concn (% w/v)	% IO adsorbed	final eq IO concn (% w/v)	specific adsorption (mg IO/g sand)	% monolayer
$PAMPS_1$ IO NPs	0.003	77.03	0.0007	1.16 ± 0.39	0.225
	0.01	95.43	0.0005	4.77 ± 1.01	0.927
	0.1	10.84	0.0891	5.42 ± 1.18	1.053
$PAMPS_2$ IO NPs	0.003	99.5	0.00002	1.49 ± 0.41	0281
	0.01	36.98	0.0063	1.85 ± 0.44	0.349
	0.1	6.78	0.0932	3.39 ± 0.69	0.639
$PAMPS_3$ IO NPs	0.003	79.70	0.0006	1.20 ± 0.33	0.235
	0.01	26.95	0.0073	1.35 ± 0.32	0.264
	0.1	5.66	0.0943	2.83 ± 0.58	0.555
$PAMPS_4$ IO NPs	0.003	78.97	0.0006	1.19 ± 0.34	0.189
	0.01	25.80	0.0074	1.29 ± 0.34	0.205
	0.1	2.90	0.0971	1.45 ± 0.51	0.231

[a]The specific surface area of crushed Berea sandstone was measured to be ~1.5 m^2/g.

Table 3. Adsorption of PMPDSA Grafted IO NPs on Silica Microspheres and Crushed Berea Sandstone in API Brine at pH 8 at Varying IO Concentrations

medium	initial IO concn (% w/v)	% IO adsorbed	final eq IO concn (% w/v)	specific adsorption (mg IO/m^2)	% monolayer
silica microspheres	0.003	0.67	0.00298	0.0010 ± 0.01	0.0001
	0.01	4.75	0.00952	0.016 ± 0.01	0.003
crushed Berea sandstone	0.003	13.39	0.00260	0.200 ± 0.040	0.076
	0.01	9.55	0.00905	0.470 ± 0.230	0.180

to be 32% at 600 °C (Figure S4). In addition, DLS data revealed a D_H of ~174 ± 30 nm(Figure S5).

The PMPDSA IO NPs were found to form stable dispersions in API brine at room temperature and at 90 °C, similar to the case of the $PAMPS_{1-4}$ IO NPs. The stability was corroborated by measuring the D_H in API brine at 90 °C for 1 week over which it remained constant at 174−185 nm, Figure S6. Collectively, these data demonstrated that the PMPDSA IO NPs were stable and only minor aggregation occurred. To the best of our knowledge, these results constituted the first demonstration of zwitterionic polymers stabilized IO NPs at high salinity and elevated temperatures over relatively prolonged time.

Static batch adsorption of PMPDSA IO NPs: Another series of adsorption tests using silica microspheres and crushed Berea sandstone were performed using PMPDSA IO NPs at different feed IO concentrations of 0.003 and 0.01% w/v in API brine (Table 3). The specific adsorption in API brine of the PMPDSA IO NPs (0.01% w/v) was 0.016 ± 0.01 mg/m^2, which corresponded to a very low NP monolayer coverage of 0.003%. As seen from Table 3, the specific adsorption was on the same order of magnitude as that of $PAMPS_{2-4}$ IO NPs on the silica microspheres.

Although on the silica microspheres the specific adsorption was the same when comparing the $PAMPS_{2-4}$ IO NPs versus the PMPDSA IO NPs, different results were observed for the crushed Berea sandstone. As seen in Table 3, an order of magnitude decrease is evident at 0.003 as well as 0.01% w/v concentrations for the PMPDSA IO NPs. These remarkable finding indicate that the zwitterionic PMPDSA coatings drastically decreases the adsorption to the crushed Berea sandstone, likely as a consequence of weaker interactions with the local cationic sites on the clay edges.

In conclusion, a facile "grafting through" approach was developed to tether tunable quantities of PAMPS and PMPDSA stabilizer to functionalized IO NP surfaces. With this method, it was possible to graft homopolymer stabilizers unlike previous "grafting to" approaches that required copolymers containing anchor groups. Not only were the PAMPS as well as PMPDSA IO NPs colloidally stable at high

dx.doi.org/10.1021/mz5004213 | ACS Macro Lett. 2014, 3, 867−871

salinities and temperatures (90 °C), but also exhibited extremely low adsorption on silica microparticles and crushed Berea sandstone. The adsorption decreased with the polymer loading for PAMPS series, whereby the particle-surface electrosteric repulsion increased. The zwitterionic PMPDSA IO NPs displayed superior properties, that is, 1 order of magnitude less adsorption to the crushed Berea sandstone relative to the anionic PAMPS IO NPs. To the best of our knowledge, these are the first examples of realizing colloidal stability and low mineral adsorption of IO NPs at high ionic strength and elevated temperatures using a zwitterionic polymer as stabilizing agent. Future efforts will focus on using NPs for applications in enhanced oil recovery,[39] environmental remediation,[35,40,41] CO_2 sequestration,[42] and electromagnetic imaging of oil reservoirs.

■ ASSOCIATED CONTENT

Supporting Information

Materials, further details in experimental procedure, and DLS, TGA, and ATR-IR of IO NPs. This material is available free of charge via the Internet at http://pubs.acs.org.

■ AUTHOR INFORMATION

Corresponding Author

*E-mail: kpj@che.utexas.edu.

Author Contributions

‡These authors contributed equally (E.F. and Z.X.).

Notes

The authors declare no competing financial interest.

■ ACKNOWLEDGMENTS

This work was supported by the Advanced Energy Consortium. Member companies include Shell, Petrobras, Schlumberger, BP America Inc., Statoil, Total, theBG Group, and Repsol. C.W.B. and K.P.J. are grateful to the Welch Foundation (F-1621 and F-1319, respectively) for support and the Gulf of Mexico Research Initiative. K.P.J. acknowledges support from NSF (CBET-1247945.)

■ REFERENCES

(1) Bagaria, H. G.; Yoon, K. Y.; Neilson, B. M.; Cheng, V.; Lee, J. H.; Worthen, A. J.; Xue, Z.; Huh, C.; Bryant, S. L.; Bielawski, C. W.; Johnston, K. P. *Langmuir* **2013**, *29*, 3195.

(2) Bagaria, H. G.; Xue, Z.; Neilson, B. M.; Worthen, A. J.; Yoon, K. Y.; Nayak, S.; Cheng, V.; Lee, J. H.; Bielawski, C. W.; Johnston, K. P. *ACS Appl. Mater. Interfaces* **2013**, *5*, 3329.

(3) Xue, Z.; Foster, E.; Wang, Y.; Nayak, S.; Cheng, V.; Ngo, V. W.; Pennell, K. D.; Bielawski, C. W.; Johnston, K. P. *Energy Fuels* **2014**, *28*, 3655.

(4) Bagaria, H. G.; Neilson, B. M.; Worthen, A. J.; Xue, Z.; Yoon, K.; Cheng, V.; Lee, J. H.; Velagala, S.; Huh, C.; Bryant, S. L.; Johnston, K. P. *J. Colloid Interface Sci.* **2013**, DOI: 10.1016/j.jcis.2013.03.012.

(5) Laurent, S.; Forge, D.; Port, M.; Roch, A.; Robic, C.; Vander Elst, L.; Muller, R. N. *Chem. Rev.* **2008**, *108*, 2064.

(6) Jeong, U.; Teng, X.; Wang, Y.; Yang, H.; Xia, Y. *Adv. Mater.* **2007**, *19*, 33.

(7) Kotsmar, C.; Yoon, K. Y.; Yu, H.; Ryoo, S. Y.; Barth, J.; Shao, S.; Prodanovicì, M.; Milner, T. E.; Bryant, S. L.; Huh, C.; Johnston, K. P. *Ind. Eng. Chem. Res.* **2010**, *49*, 12435.

(8) Ryoo, S.; Rahmani, A. R.; Yoon, K. Y.; Prodanovic, M.; Kotsmar, C.; Milner, T. E.; Johnston, K. P.; Bryant, S. L.; Huh, C. *J. Pet. Sci. Eng.* **2012**, *81*, 129.

(9) Park, Y. C.; Paulsen, J.; Nap, R. J.; Whitaker, R. D.; Mathiyazhagan, V.; Song, Y.-Q.; Hürlimann, M.; Szleifer, I.; Wong, J. Y. *Langmuir* **2014**, *30*, 784.

(10) Kadhum, M. J.; Swatske, D. P.; Harwell, J. H.; Shiau, B.; Resasco, D. E. *Energy Fuels* **2013**, *27*, 6518.

(11) McCormick, C. L.; Elliott, D. L. *Macromolecules* **1986**, *19*, 542.

(12) Newman, J. K.; McCormick, C. L. *Macromolecules* **1994**, *27*, 5114.

(13) Goda, T.; Watanabe, J.; Takai, M.; Ishihara, K. *Polymer* **2006**, *47*, 1390.

(14) Sun, Q.; Su, Y.; Ma, X.; Wang, Y.; Jiang, Z. *J. Membr. Sci.* **2006**, *285*, 299.

(15) Lowe, A. B.; Billingham, N. C.; Armes, S. P. *Macromolecules* **1999**, *32*, 2141.

(16) Cheng, G.; Li, G.; Xue, H.; Chen, S.; Bryers, J. D.; Jiang, S. *Biomaterials* **2009**, *30*, 5234.

(17) Johnson, K. M.; Fevola, M. J.; Lochhead, R. Y.; McCormick, C. L. *J. Appl. Polym. Sci.* **2004**, *92*, 658.

(18) Noh, J.-G.; Sung, Y.-J.; Geckeler, K. E.; Kudaibergenov, S. E. *Polymer* **2005**, *46*, 2183.

(19) Vaisocherova, H.; Zhang, Z.; Yang, W.; Cao, Z.; Cheng, G.; Taylor, A. D.; Piliarik, M.; Homola, J.; Jiang, S. *Biosens. Bioelectron.* **2009**, *24*, 1924.

(20) Yang, W.; Xue, H.; Carr, L. R.; Wang, J.; Jiang, S. *Biosens. Bioelectron.* **2011**, *26*, 2454.

(21) Sakai-Kato, K.; Kato, M.; Ishihara, K.; Toyo'oka, T. *Lab Chip* **2004**, *4*, 4.

(22) Goda, T.; Ishihara, K. *Expert Rev. Med. Devices* **2006**, *3*, 167.

(23) Suzuki, S.; Saimi, Y.; Ono, T. *J. Biomed. Mater. Res., Part B* **2006**, *76B*, 184.

(24) Kimura, M.; Takai, M.; Ishihara, K. *J. Biomed. Mater. Res., Part A* **2007**, *80A*, 45.

(25) Sun, J.-T.; Yu, Z.-Q.; Hong, C.-Y.; Pan, C.-Y. *Macromol. Rapid Commun.* **2012**, *33*, 811.

(26) Jiang, S.; Cao, Z. *Adv. Mater.* **2010**, *22*, 920.

(27) Li, G.; Cheng, G.; Xue, H.; Chen, S.; Zhang, F.; Jiang, S. *Biomaterials* **2008**, *29*, 4592.

(28) Gao, C.; Li, G.; Xue, H.; Yang, W.; Zhang, F.; Jiang, S. *Biomaterials* **2010**, *31*, 1486.

(29) Barbey, R.; Lavanant, L.; Paripovic, D.; Schuwer, N.; Sugnaux, C.; Tugulu, S.; Klok, H.-A. *Chem. Rev.* **2009**, *109*, 5437.

(30) Zhang, Z.-H.; An, Q.-F.; Liu, T.; Zhou, Y.; Qian, J.-W.; Gao, C.-J. *Desalination* **2012**, *297*, 59.

(31) Frickel, N.; Messing, R.; Gelbrich, T.; Schmidt, A. M. *Langmuir* **2009**, *26*, 2839.

(32) Tsubokawa, N.; Kimoto, T.; Koyama, K. *Colloid Polym. Sci.* **1993**, *271*, 940.

(33) Foster, E. L.; Tria, M. C. R.; Pernites, R. B.; Addison, S. J.; Advincula, R. C. *Soft Matter* **2012**, *8*, 353.

(34) Pernites, R. B.; Foster, E. L.; Felipe, M. J. L.; Robinson, M.; Advincula, R. C. *Adv. Mater.* **2011**, *23*, 1287.

(35) Petosa, A. R.; Jaisi, D. P.; Quevedo, I. R.; Elimelech, M.; Tufenkji, N. *Environ. Sci. Technol.* **2010**, *44*, 6532.

(36) Wever, D. A. Z.; Picchioni, F.; Broekhuis, A. A. *Prog. Polym. Sci.* **2011**, *36*, 1558.

(37) Wielema, T. A.; Engberts, J. B. F. N. *Eur. Polym. J.* **1987**, *23*, 947.

(38) Hirasaki, G. J.; Miller, C. A.; Raney, O. G.; Poindexter, M. K.; Nguyen, D. T.; Hera, J. *Energy Fuels* **2009**, *25*, 555.

(39) Ponnapati, R.; Karazincir, O.; Dao, E.; Ng, R.; Mohanty, K. K.; Krishnamoorti, R. *Ind. Eng. Chem. Res.* **2011**, *50*, 13030.

(40) Saleh, N.; Kim, H.-J.; Phenrat, T.; Matyjaszewski, K.; Tilton, R. D.; Lowry, G. V. *Environ. Sci. Technol.* **2008**, *42*, 3349.

(41) Wang, Y.; Li, Y.; Fortner, J. D.; Hughes, J. B.; Abriola, L. M.; Pennell, K. D. *Environ. Sci. Technol.* **2008**, *42*, 3588.

(42) Javadpour, F.; Nicot, J.-P. *Transp. Porous Media* **2011**, *89*, 265.